The nano-magnetite-loaded 2-mercaptobenzoxazole as an adsorbent for the selective removal of the Pb²⁺, Ni²⁺ and Cd²⁺ ions from aqueous solutions

Maryam Ariannezhad*,†, Davood Habibi*, Somayyeh Heydari*,**, and Vahideh Khorramabadi*

*Department of Organic Chemistry, Faculty of Chemistry, Bu-Ali Sina University, Hamedan, 6517838683, Iran
**Department of Research and Development of the Faran Shimi Pharmaceutical Company, Tuyserkan, Iran

Abstract−The present research focuses on the adsorption efficiency of nano-magnetite loaded 2-mercapto- benzoxazole as an adsorbent (Fe_3O_4@SiO_2@CPTMS@MBOL) for Pb^{+2}, Ni^{+2} and Cd^{+2} removal from the contaminated water by the technique of adsorption. The influence of pH, contact time, adsorbent dosage and temperature in 50 ppm concentration of each ion solutions on the sensitivity of the removal procedure was examined. By ICP test the adsorption data were fixed to linearize the adsorption isotherms of the Langmuir and Freundlich equations. This efficient adsorbent showed significant results for metal ion removal from water by formation of complex with adsorbent. From the Langmuir isotherm, the maximum adsorption capacities of nano magnetic adsorbent towards Pb^{2+}, Ni^{2+} and Cd^{2+} ions were 238.4, 203.2 and 22.37 mgg^{-1}.

Keywords: Adsorption, 2-Mercaptobenzoxazole, Adsorption Isotherms, Solution Ions, Nano Magnetic

INTRODUCTION

Although the heavy metals are essential elements, but in high concentration led to severe environmental and health threats [1]. In fact, metal ions from natural phenomena like volcanic eruptions, forest fires, wind erosion or fossil fuel consumption pose less harmful environmental impacts in contrast with the metal ions from anthropogenic activities, such as urbanization, thermal power plants, mines and factories [2]. The nature of non-biodegradability of toxic metals causes them to endure living in different systems for long time and consequently hazardous threats via entering the food chain [3,4]. Recent surveys indicate that exposure to pollutants such as nickel, arsenic, cadmium and mercury could affect the epigenetic elements of the genome [5]. Existence of Pb pollution in agricultural sites will cause severe environmental difficulties, such as loss of vegetation and reduction in soil fertility. Lead is a serious poisonous metal through inducing toxicity in living organisms [6]. As is well recognized, gastrointestinal and nervous systems could be affected by lead poisoning [7]. The considerable amount of nickel in the aquatic environment in accordance with its high application in various productive sectors provides ingestion of nickel in excess of recommended levels that causes pulmonary fibrosis, lung and dermatological diseases [8]. Cadmium contamination mainly has consequences through electroplating and paint industries, batteries and zinc mines. Affinity of bioaccumulation and having long half-life (10-33 years) in the human body reveals the hazard of cadmium on liver and kidney obviously [9]. Many attempts have been done to remove or at least decrease the concentration of different metal ions from water samples [10]. According to World

Health Organization (WHO), the level of contamination of lead, nickel and cadmium in drinking water should not be beyond 0.05 mg/dm^3 [11].

Due to persisting contaminated water via increased population and industrial effluents, there are different approaches for metal removal from water resources. The use of unique, alternative and low-cost adsorbent is one of the most challenging issues [12]. Although there are several available technologies for removing heavy metal ions from water, such as chemical ion exchange [13], precipitation [14], nano-filtration [15], reverse osmosis [16], adsorption by interfacing solid-solution is an important method for reduction of pollutants of heavy metal ions [17]. Activated carbon method is not cost-effective for developing countries [18]. Natural inorganic zeolites [19] and clay [20] suffer from low capacity, easy separation and weak binding affinity for heavy metal ions. These problems cause discovering materials that are both efficient and low-priced. The use of magnetic Fe_3O_4 is widely spread out to the practical adsorption of different chemical sorts from water via chemical modification of surface of nanoparticles [21,22]. Several strategies have been reported due to functionalization of magnetic nanoparticles via different organic groups containing donor atoms which have ability of selective interaction with specific metal ions. On the other
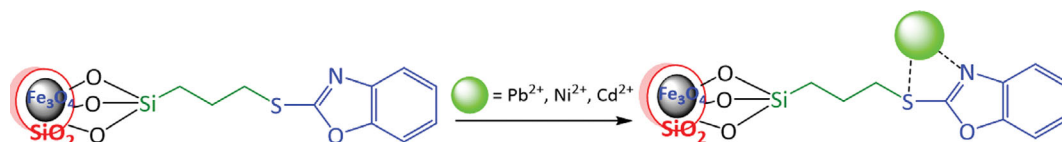
†To whom correspondence should be addressed.
E-mail: mary.ariannezhad@yahoo.com
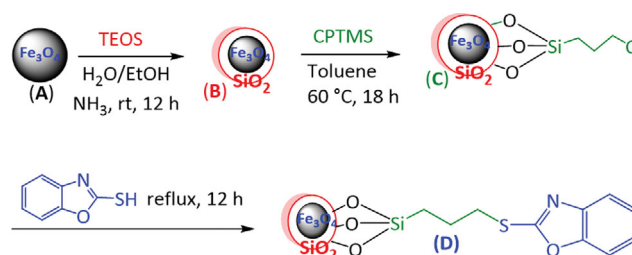
Scheme 1. Synthesis of Fe_3O_4@SiO_2@CPTMS@MBOL.

Scheme 2. Removal of Pb⁺², Ni⁺² and Cd⁺² from the water by nano-adsorbent.

hand, decrease of particle size, large surface area could lead to greater adsorption capacity permitting for smaller sorbent volumes [23,24].

According to the characters of toxicity and carcinogenic agents of heavy metal ions such as lead, cadmium and nickel at even low concentrations [25], reliable methods are essential for the removal of heavy metals from environmental matrices. In this work, with an attempt to make improvements to the metal complexing ability, Fe_3O_4 nanoparticle surface was modified with organic ligands used as simple, separable and recyclable nano adsorbent for the efficient removal of these metal ions from contaminated water. Herein, we wish to report synthesis of the nano magnetic adsorbent modified with 2-mercaptobenzoxazole to adsorb the Pb²⁺, Ni²⁺ or Cd² ions from aqueous solutions by formation of the corresponding complexes and investigation of the maximum adsorption capacity (Schemes 1 and 2). The experimental parameters of removal processes such as the adsorbent dosage, pH, contact times and temperature were optimized as well.

EXPERIMENTAL

1. Reagents and Materials

All chemicals (starting materials, reagents, solvents…) were pre-pared from the Merck and Aldrich chemical companies and used without additional purification.

2. Preparation of the Adsorbent

The nano-magnetite adsorbent was prepared according to the procedure described before [26].

Fe_3O_4 MNPs were formed by the mixing of $FeCl_3 \cdot 6H_2O$ (11.44 g) and $FeCl_2 \cdot 4H_2O$ (4.3 g) in 100 mL distilled water under stirring conditions for 40 minutes at 70 °C, and then after adding aqueous ammonia (37%) slowly, the pH reached to 10 and a black precipitate was obtained and in the following the mixture was heated about 35 minutes at 70 °C. Fe_3O_4 magnetic nanoparticles were separated by external super magnet, washed by water three times and dried at 70 °C for 24 h. In the second step 0.1-g of Fe_3O_4 MNPs was added in a mixture of ethanol, distilled water (100 mL, 4 : 1 by volume) and aqueous ammonia (2 mL) and dispersed under ultrasonication for 10 minutes. Afterward Tetraethyl orthosilicate (2 mL) was slowly added and the mixture was stirred for 8 h. The obtained solid was filtered by centrifugation, washed with ethanol and water and dried in vacuo. In the third step for the functionalization, the coated Fe_3O_4 was added to the mixture of 3-Chloropropyl(trimethoxy)silane (1 ml, 5 mmol) dissolving in anhydrous toluene (80 mL) and the mixture was stirred for 18 h at 60 °C; the resulting solid as in previous steps was separated and dried. At the final step in a round flask (100 ml) containing a reflux condenser the reactions of previous step product (0.1 g) with 2-mercapto-benzoxazole (0.75 g, 5 mmol), potassium carbonate (0.69 g, 5 mmol) in toluene (50 mL) was carried out. At the end, the product was washed repeatedly with ethanol and water and dried under reduced pressure.
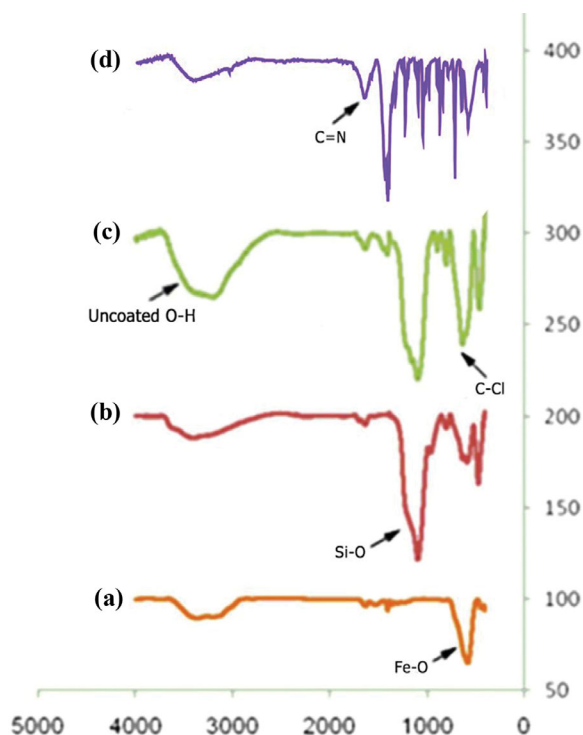

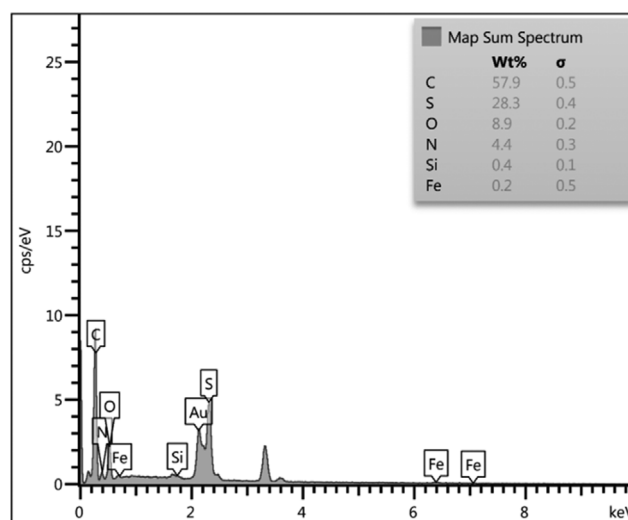**Fig. 1. Comparative FT-IR spectra of four steps ((a), (b), (c) and (d)).**

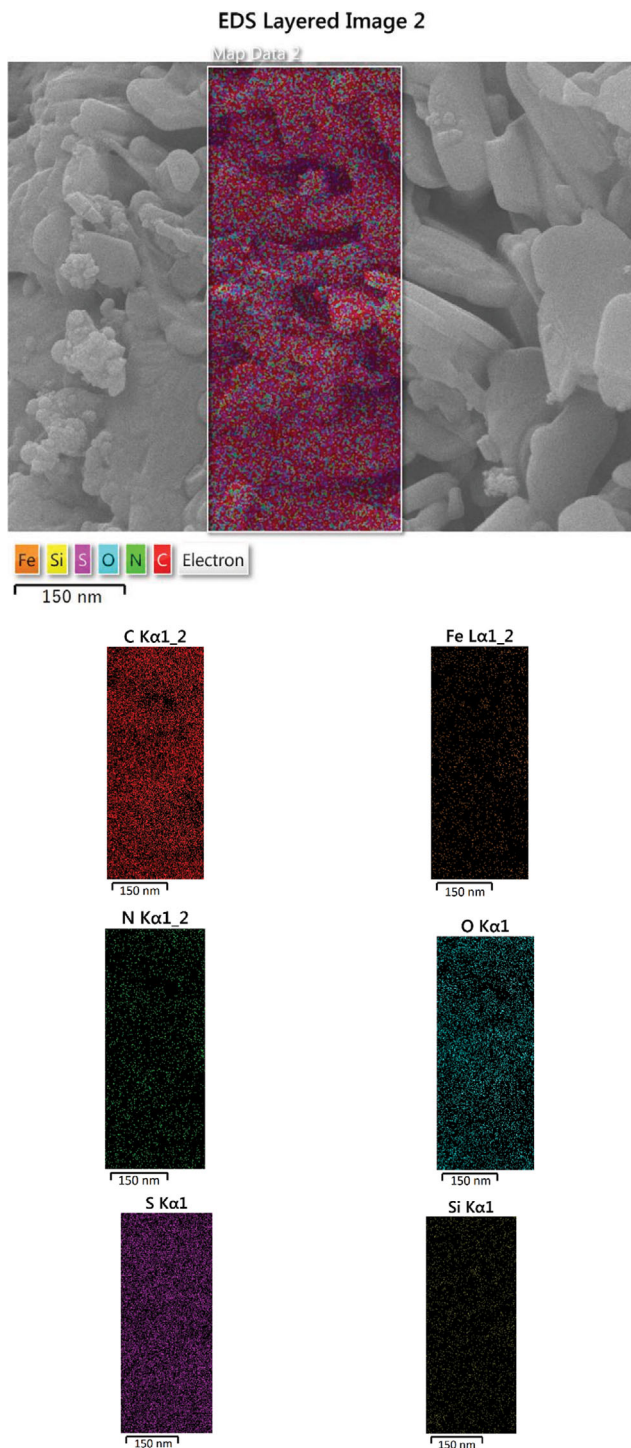**Fig. 2. The EDX analysis of the adsorbent (Fe₃O₄@SiO₂@CPTMS@ MBOL).**

Fig. 3. The elemental mappings of the adsorbent (Fe₃O₄@SiO₂@ CPTMS@MBOL).

Fig. 4. The XRD pattern of the adsorbent (Fe₃O₄@SiO₂@CPTMS@ MBOL).

RESULTS AND DISCUSSION

1. Characterization of the Nano-magnetite Adsorbent

The structure of adsorbent was confirmed by different below techniques.

2. FT- IR Spectroscopy Analysis

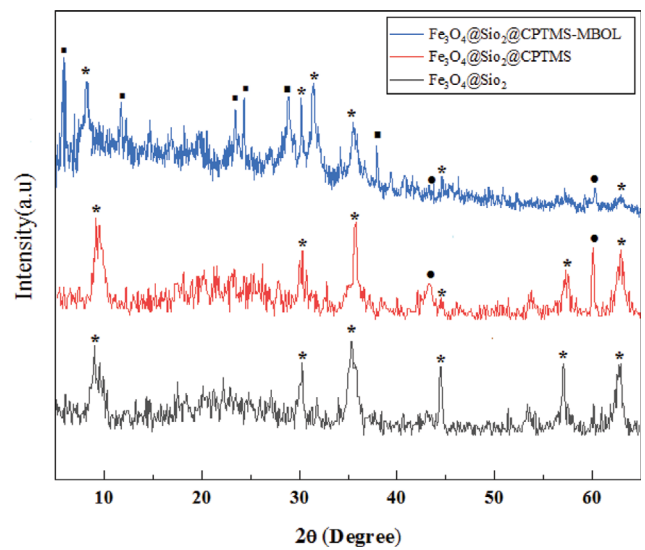Due to (Fig. 1) preparation of Fe_3O_4 MNPs in the step of (a) was characterized through a peak at about 578 cm^{-1} which is corresponding to the stretching vibrations of Fe-O. In the second step (b) formation of $Fe_3O_4@SiO_2$ was detected by a wide peak nearby 1,087 cm^{-1} which revealed coating of silica with magnetite nanoparticles. In third step (c) a new peak at about 581 cm^{-1} indicates C-Cl bond. Finally, in the step (d) appearing of two newly discovered peaks at 1,345 and 1,664 cm^{-1} are associated with the C-N and C=N bonds, consecutively.

3. EDX and Mapping Analysis

EDX and mapping elemental analysis (Figs. 2 & 3) indicates chemical composition of the nano adsorbent. The results ratify the existence of the suggested elements in the construction of the adsorbent, including C, N, O, Si, S, and Fe. Normally, a very thin layer of gold was coated with the compound that leads to existence of the Au peak in the EDX graph analysis, as well.

4. XRD Patterns of the Nano-adsorbent

According to appraisement of the crystallographic features of $Fe_3O_4@SiO_2@CPTMS@MBOL$, XRD analysis was performed for $Fe_3O_4@SiO_2$ (grey, **A**), $Fe_3O_4@SiO_2@CPTMS$ (red, **B**) and $Fe_3O_4@SiO_2@CPTMS@MBOL$ (blue, **C**) and shown in Fig. 4. The diffraction peaks at 2θ=10, 30, 35, 45, 53, 57 and 63 exhibit the cubic spinel crystal planes of Fe_3O_4 could be effectively coated by silica. The characteristic peaks associated with the ligand group appeared around 2θ=7, 12, 23, 24, 29, 37, which some of them were overlaid with the Fe_3O_4 diffraction peaks. Particle size was calculated by using Debye Scherrer formula about 17.67 nm.

5. SEM Analysis of Nano-adsorbent

Morphological characteristics of the prepared adsorbent were investigated by SEM analysis. The SEM images of $Fe_3O_4@SiO_2$-CPTMS-MBOL shown in Fig. 5 indicate nanometer dimensions of adsorbent and exhibit uniform and spherical morphology, and the formation of sintered grains with the 19.9-46.8 nm size range was apparent.

6. VSM Technique for the Nano-adsorbent

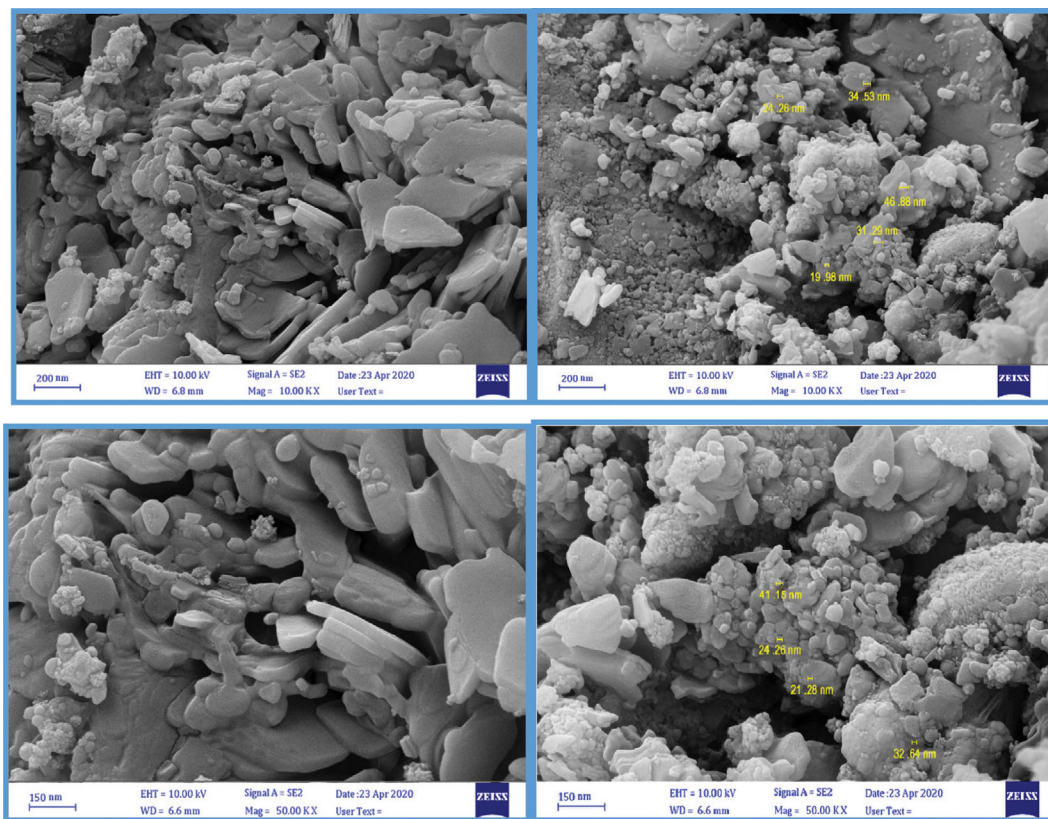According to a comparative evaluation for the magnetic proper-

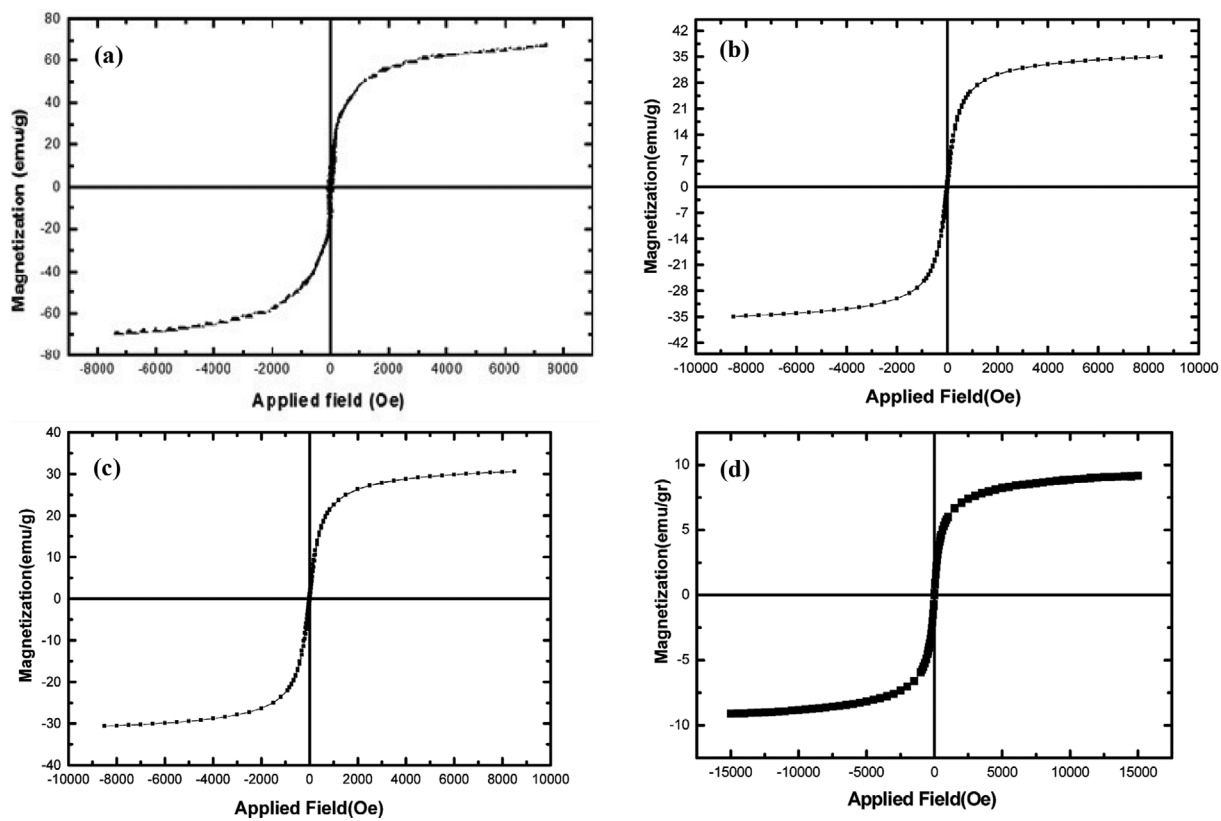Fig. 5. The SEM images of the adsorbent (Fe₃O₄@SiO₂@CPTMS@MBOL).

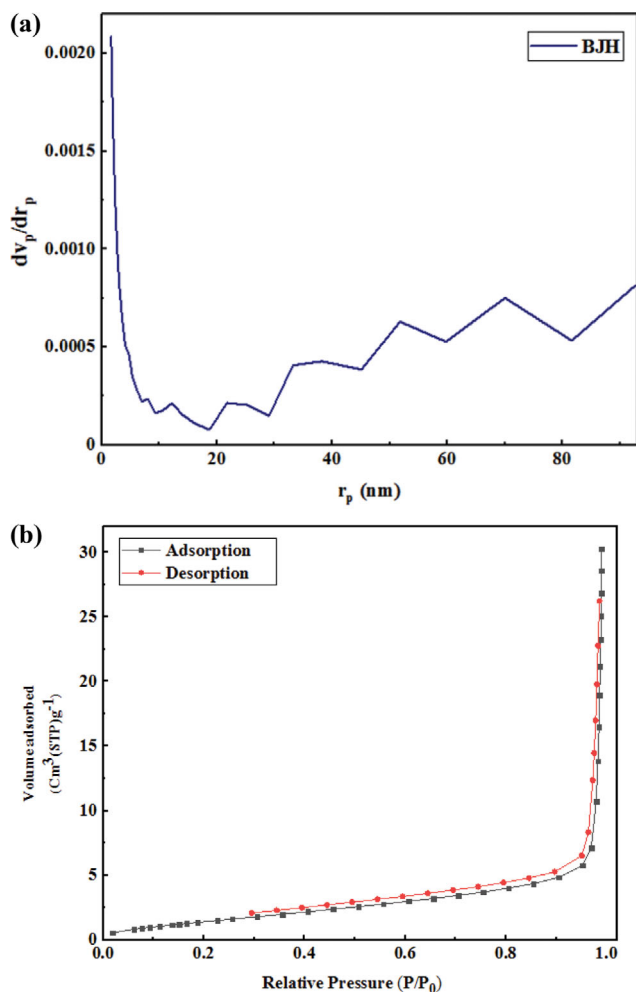Fig. 6. The VSM analysIs of (a), (b), (c) and (d).

(a)

(b)

Fig. 7. (a) The N₂ gas adsorption- desorption isotherm for the magnetic nano adsorbent. (b) BET pore size distribution for the magnetic nano adsorbent.

Table 1. Results of the Langmuir and BET measurements of nano adsorbent

Parameter	Langmuir	BET
a_s (m²/g)	8.2	6.24
V_m (cm³(STP) g⁻¹)	1.9	1.43

Table 2. Results of volume and radius of cavities using different experimental isotherms

Methods	Pore volume (cm³/g)	Pore size (nm)	a_p (m²/g)
BJH method adsorption	0.047	1.22	6.95
BJH desorption	0.045	1.66	4.65
DH	0.047	1.22	7.43
SF	0.045	1.66	4.62
αs	0.001	-	3.44
Total pore volume	0.046 cm³/g		
Mean pore diameter	29.85 nm		

Barrett-Joyner-Halenda Method (BJH), Dollimore Heal Method (DH), Saito-Foley Method (SF), Alpha S Method (αs)

ties, the VSM analysis was accomplished for the each step of preparing of the adsorbent including (a) Fe₃O₄ MNPs, (b) Fe₃O₄@SiO₂, (c) Fe₃O₄@ SiO₂-CPTMS, (d) Fe₃O₄@SiO₂@CPTMS@MBOL (Fig. 6). Generally, all steps of formation show magnetic possessions and a noticeable decrease from (a) to (d) (65, 35, 30, 10 and 4.35 emu/g, respectively) would be observed. In fact, the dipolar-dipolar interactions reduce between the magnetic nanoparticles due to coating of Fe₃O₄ MNPs via different layers.

7. Characterization of Nano Adsorbent by the BET Measurements

To obtain the specific surface area, nitrogen uptake and desorption and total pore volume analysis was performed at 77 Kelvin (Fig. 7(a), (b)). According to IOPAC classification, adsorption and desorption isotherms, the system is type 4 isotherm and type 3 hysteresis, which indicates the interaction between adsorbent and pollutants is very low. Also, due to the presence of hysteresis in the adsorbent isotherm, meso-cavities and cavities are grooved, flexible and expandable. BJH results show the distribution of pores. Although the pore accumulation is in the range of 1 nm, there are pores from the micro pore to the meso porous range and hetero-

geneous distribution of pores in the structure. In fact, the type of isotherm is evidence of this. According to the Langmuir adsorption isotherm, the specific surface area of the adsorbent is 8.2 m²g⁻¹ and the volume of adsorbed nitrogen gas is 1.9 cm³ g⁻¹ (Table 1). The results were inspected with other experimental isotherms for nitrogen uptake and desorption and presented in Table 2. Based on the results, the total volume of cavities is equal to 0.046 nm and the average diameter of cavities is 29.82 nm. Due to the core-shell structure of the adsorbent, this special surface has a low surface in comparison with commercial adsorbents, and it can be said that the adsorption of pollutants has been done physically, chemically and in a single layer.

8. Adsorption Experiments

Due to evaluation of adsorption tests, 0.025 g of the adsorbent was used for every 35 ml solution of Pb²⁺, Ni²⁺ and Cd⁺² in concentrations of 50, 150 and 200 mg/l. Then Erlenmeyer flasks were stirred at 180 rpm for 2 hours at room temperature (25 °C). After stirring, the contents of the Erlenmeyer flasks were centrifuged at 1,000 rpm for 20 minutes to separate the solid and liquid phases. The isolated liquids were sent to the ICP analysis. Finally, adsorption kinetics, adsorption isotherms, pH, temperature and amount of adsorbent were investigated. The results show that the initial level of pollutant is one of the most important parameters affecting the adsorption process. The concentration of heavy metals in different waters and wastewaters is variable, which causes to change the rate of separation of the adsorption process. This can be due to the delay in a balance between the adsorbent and the contaminant. Because the amount of adsorbent is constant through the process, the amount of active sites is constant too. Among the increasing the amount of pollutants, active sites are fixed so saturation of these sites will happen and the percentage of adsorption decrease. In general, as the initial concentration of the contaminant increases, the removal percentage decreases. As a

Table 3. The concentration of Ni^{2+}, Cd^{2+} and Pb^{2+} before and after adsorption by the absorbent (reported by ICP)

Conct. of Ni^{2+} (ppm)		%Adsp. Ni^{2+}	Conct. of Pb^{2+} (ppm)		%Adsp. Pb^{2+}	Conct. of Cd^{2+} (ppm)		%Adsp. Cd^{2+}
Before	After		Before	After		Before	After	
45.5	1.5925	96.5	50	0.0455	99.9	50	15.197	66.6
150	101.4676	32.4	150	15.1601	89.9	150	88.559	41
200	120.3098	41.14	200	49.4648	75.8	200	129.1808	36.8

result of the concentration of 50 mg/l was selected for the experiments of this study (Table 3).

The amount of metal adsorption on the adsorbent (adsorption capacity) is denoted on q. The values of q were calculated using the following equation. q is the adsorption capacity in terms of (mg/g), C_0 is the initial concentration of pollutants in terms of (mg/L), C_e is the equilibrium concentration of pollutants in terms of (mg/L), V is volume in liters and m is the amount of adsorbent used in the experiment.

$$q = \frac{(C_0 - C_e) \times V}{m}$$

9. Effect of the pH

The pH of the solution is one of the most important factors influencing the absorption process and the mechanism of electrostatic forces. To determine the most suitable pH and the effect of that on the adsorption performance, Pb^{2+}, Ni^{2+} and Cd^{2+} solutions were evaluated in the concentration of 50 mg/l with 0.025 g of adsorbent in the pH changed between 5-9 ranges via using either 0.1 M NaOH or 0.1 M HCl for the pH adjustment. Surface charge properties of adsorbent can be studied from the point of zero charge (PZC) measurements which obtained 8 for the nano adsorbent [27]. The pH PZC of adsorbent was measured by drift method. pH PZC is pH when the charge in the adsorbent surface is zero. At pHs less than the PZC, the surface charge of the adsorbent is positive and at pHs higher than the PZC the surface charge is negative. The -OH functional groups on adsorbent increases the acidity of the adsorbent. Acidic pH causes protonation of C-N and Si-O groups, so high concentration of these functional groups causes positive adsorption surface charge [28]. At pHs higher than 7.5, the adsorbent and Pb^{+2} have the same surface charge and electrostatic force is established between them. Due to the absorption capacity, the dominant mechanism is ion exchange. At lower pHs, adsorbent and pollutant have the same surface charge and repel each other. As a result, changing the pH has no effect on lead adsorption and the main mechanism is ion exchange. For nickel and cadmium, their positive surface charge and the PZC of adsorbent, at pH 8, is due to the anonymity of adsorbent surface charge (negative) and pollutant (positive), the maximum amount of adsorption are (61.7 and 47.1 mgg^{-1}, respectively). Also, at pHs less than 7, due to the same surface charge of adsorbent (positive) and pollutant (positive), the amount of adsorption decreases and the effect of electrostatic forces decreases and ion exchange mechanism is the dominant mechanism. According to formation of colloidal sediment at base pHs the concentration of cadmium in aqueous solution decreases and consequently adsorption capacity decreases at pH more than 8. However, at pH 8, the highest amount of ad-
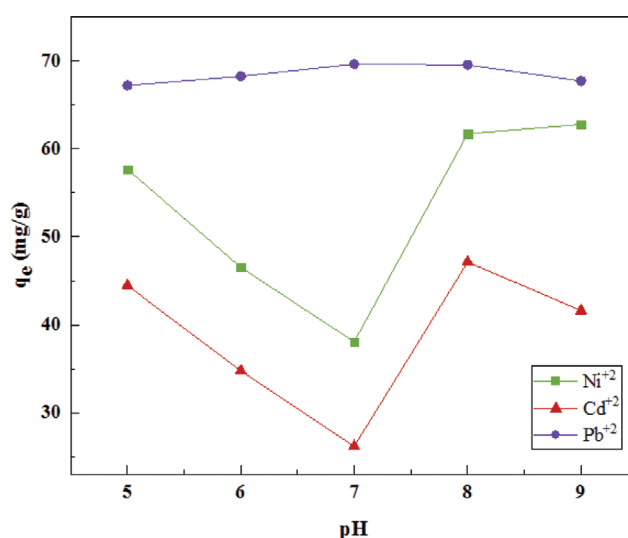

Fig. 8. The effect of pH on the adsorption capacity (Initial concentration of ions: 50 mg/l, weight of adsorbent: 0.025 g, solution volume: 35 mL, r.t, contact time 120 min).

sorption occurs due to the uneven surface charge of the pollutant and adsorbent. The effect of pH on the adsorption capacity is shown in Fig. 8.

According to Fig. 8 and results, pH 8 was selected as the optimal pH for the next experiments due to the maximum adsorption capacity of all three pollutants.

10. Effect of the Amount of the Adsorbent

To evaluate the amount of optimal adsorbent, different amounts of adsorbent 0.025, 0.05, 0.1, 0.125 and 0.15 g in 35 ml of solution with initial concentration of Pb^{2+}, Ni^{2+} and Cd^{2+} 50 mg/l, pH 8 and duration of 120 minutes were investigated. As can be seen in Fig. 9, with increasing the amount of adsorbent from 0.025 to 0.15 g, the q$_e$ decreased from 69.6, 53.3 and 45.7 to 14 (mgg^{-1}) for Pb^{2+}, Ni^{2+} and Cd^{2+}, respectively due to the adhesion and agglomeration of the adsorbent and the decrease of the available active surface. Therefore, in subsequent experiments the optimal amount of adsorbent 0.025 g in 50 ml of aqueous solution was considered.

11. Effect of the Temperature

According to Fig. 10, as the temperature increases, the velocity of the dissolved ions increases and as a result they find enough energy to be adsorbed on the surface of adsorbent, so the adsorption process is more efficient at high temperatures. Due to the lack of noticeable difference in adsorption capacity at temperatures and energy consumption for higher temperatures, the room temperature °C was selected for the experiments.
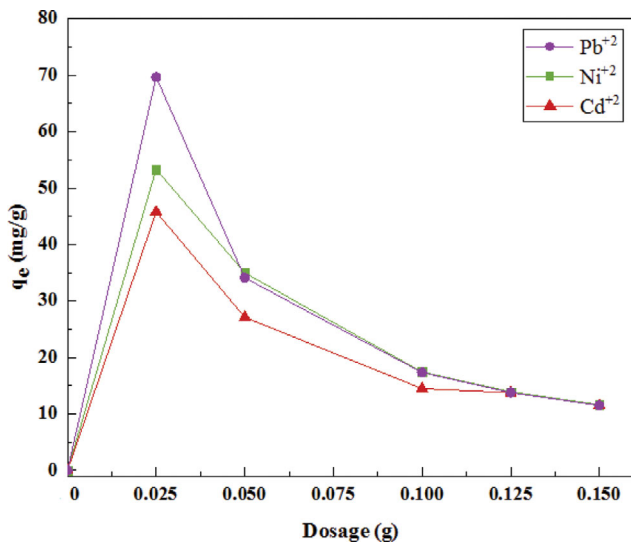
Fig. 9. The effect of amount of adsorbent on the removal of metal ions (Initial concentration of ions: 50 mg/*l*, PH8, solution volume: 35 mL, r.t, contact time: 120 min).
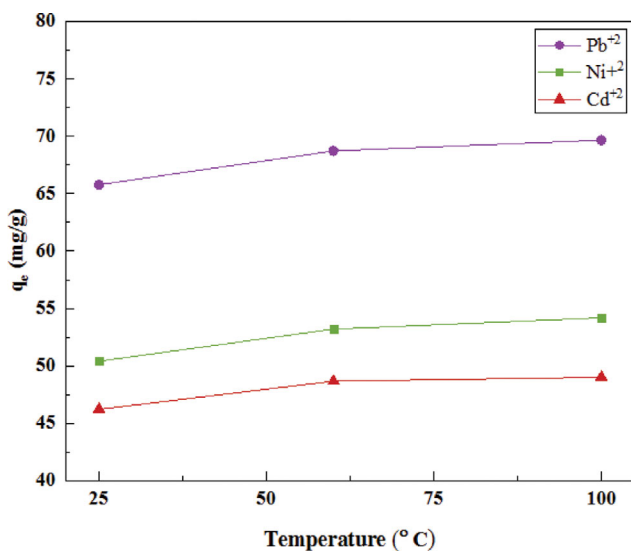
Table 4. Constants and coefficients related to adsorption kinetic models

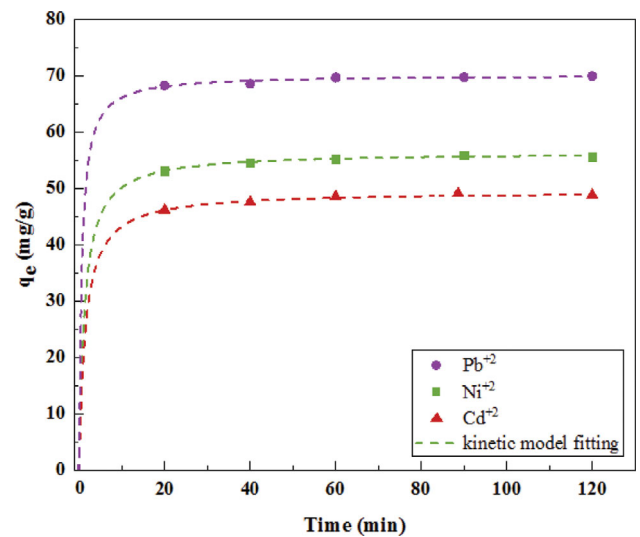| Model	Parameter	Ni	Cd	Pb
First-order quasi-linear	q_e (mg·g^{-1})	55.56	47.99	69.54
	K_1 (min^{-1})	0.15	2.17	0.20
	R^2	0.99	0.99	0.99
Second-order quasi-linear	q_e (mg·g^{-1})	56.7	49.52	70.22
	$K_2/10^{-2}$ (g/(mg·min))	0.012	0.013	0.023
	R^2	0.99	0.99	0.99
Intraparticle penetration	C (mg/g)	14.57	12.69	18.99
	k_{ipd} (mg·min$^{-0.5}$ g^{-1})	4.81	4.2	5.96
	R^2	0.70	0.71	0.68
Elovich	β (g/mg)	0.1533	0.1693	0.2409
	α (mg/g·min)	7632	5046.6	18.6*10^6

Fig. 11. Process of the second-order quasi-linear kinetic model for Pb^{+2}, Ni^{+2} and Cd^{+2} adsorption (Initial concentration of ions: 50 mg/*l*, solution, weight of adsorbent: 0.025 g, volume: 35 mL, contact time: 120 min, r.t).

Fig. 10. The effect of temperature on the adsorption (Initial concentration of ions: 50 mg/*l*, weight of adsorbent: 0.025 g, volume: 35 mL, r.t, contact time: 120 min).

12. Effect of Contact Time and Kinetic

Adsorption kinetics is the most important factor in designing any systems for predicting capability of adsorption. These experiments were performed to investigate the effect of contact time for adsorption of metal ions as well as to determine the equilibrium time. The solutions were prepared with an initial concentration of 50 mg/*l* and 0.025 g of adsorbent were added to them. Then they were put in a shaker at 250 rpm and 25 °C for 2 hours (to ensure equilibrium of the adsorption process). Then, at different time intervals, the adsorption rate of each sample was measured until the adsorption capacity reached a constant number or did not change much, which we called the equilibrium time. The obtained data were matched with first-order quasi-linear kinetic models, second-order quasi-linear and intraparticle diffusion model, and unknown values of kinetic models were obtained. According to Table 4 and the correlation coefficients R^2 of each model, the second-order quasi-linear model is acceptable for adsorption of nickel, cadmium and lead. The second-order quasi-linear kinetic model is based on the hypothesis that the reaction (ion exchange) is a speed limiter and that mass transfer in solution is not considered.

The Elovich model describes the chemical nature of the adsorption and is generally expressed [29] as where α is the initial adsorption rate (mg-g^{-1}-min^{-1}) and β is the Elovich constant related to the surface coverage (gmg^{-1}). α, β and correlation coefficients, are also presented in Table 4. The correlation coefficients were in the range of 0.87-0.994. The Elovich kinetic model precisely defined the adsorption process for all of the metal ions study. The coefficients α and β are related to chemisorption rate and surface coverage, respectively.

The study of intraparticle diffusion kinetics also shows the par-

Table 5. Constants and coefficients of adsorption isotherm models for nickel, cadmium and lead contaminants for nickel, cadmium and lead contaminants

Model	Parameter	Ni	Cd	Pb
Langmuir isotherm	q_{max} (mg·g^{-1})	203.2	22.37	238.4
	K_L (L·mg^{-1})	0.15	0.30	0.46
	R^2	0.99	0.97	0.99
Freundlich isotherm	K_F (mg^{1-n}·L^n·g^{-1})	49.78	10.8	105.9
	n	4.6	6.2	5.7
	R^2	0.84	0.94	0.86
Temkin isotherm	B_T (Kj·mol^{-1})	20.13	3.06	30.68
	A_T (L·mg^{-1})	8.05	16.36	25.58
	R^2	0.84	0.81	0.85
Redlich-Peterson isotherm	K_{RP} (L·mg^{-1})	31.01	5.28	112.2
	α_{RP} (L·mg^{-1})	0.10	0.17	0.32
	β_{Rp}	1.18	1.07	1.08
	R^2	0.99	0.99	0.99
Dubinin-Radushkevich (D-R) isotherm	q_{max}	119	22.13	203
	K_{DR}	$1.329*10^{-7}$	$9.08*10^{-8}$	$2.15*10^{-7}$
	R^2	0.92	0.96	0.98

ticle penetration velocity constant between 4.2-2.96 and the constant number C, which indicates the thickness of the boundary layer and indicates the transfer of external mass. This means that there is a mass transfer process on the outer surface that controls the initial stage of adsorption. On the other hand, a sharp increase in the rate of absorption in the early stages of the process is also considered as a rapid stage of initial mass transfer.

As shown in Fig. 11, in the early times, the adsorption rate was higher due to the vacancy of the active sites on the surface of adsorbent and the high initial concentration of the contaminant (the slope of the diagram is steep) and by the approaching to the equilibrium condition, adsorption sites are gradually occupied. Therefore, the speed of the adsorption process comes down (the slope of the diagram is reduced to zero) until the adsorbent has no more efficiency and the adsorption diagram becomes stable. Also, after about 30 minutes, the absorption diagram is fixed and the absorption process reaches equilibrium. However, to ensure about complete equilibrium, the study period lasted up to 2 hours.

ADSORPTION ISOTHERMS

In the adsorption process, it is important to obtain the amount of removal contaminant from the aqueous solution. In this study, Langmuir, Freundlich and Temkin isotherm models and Redlich-Patterson three-parameter model were used for evaluation of adsorption. Adsorption isotherm constants are determined to express the surface property and its affinity for the adsorption process.

Langmuir constant q_m indicates the adsorption of a single layer in equilibrium. The coefficients R^2 for nickel, cadmium and lead ions in the Langmuir model are 0.99. The K_L constant in the Langmuir model is used to express the ion adsorption power and its value is between 0.15 and 0.46. Also, the maximum adsorption capacity for lead ions is 238.4 mg/g. From the collating of the

experimental data by using the Langmuir isotherm, it was found that there is no difference between the isotherm model and the experimental adsorption capacity of the measurement, which is shown in Table 5.

The Freundlich isotherm represents adsorption at a heterogeneous level in interaction with the adsorbent. According to Table 2, the coefficient R^2 is 0.84, 0.94 and 0.86 for nickel, cadmium and lead ions, respectively, which is lower than the Langmuir isotherm. This confirmed that the Freundlich isotherm could not describe the adsorption function of these ions. K_F was determined to be 49.78, 10.8 and 105.9, respectively. The parameter n that is related to the Freundlich isotherm is an indication of the desirability of the adsorption process. For values of n between 0 and 10 according to the data in Table 2, the absorption is desirable.

The Temkin isotherm assumes that the adsorption heat decreases linearly. It is also assumed that the adsorption process is characterized by a uniform and continuous distribution of energy. According to the Table 5, the heat adsorption of metal ions decreases linearly with the surface. AT indicates the equilibrium bond and is associated with the maximum bond energy and BT is associated with the heat of adsorption. Low BT indicates a weak bond between the pollutant and adsorbent molecules.

Among the three-parameter isotherm models, the Redlich-Peterson model is often used to adsorb the liquid phase of heavy metals and organic compounds. According to the obtained correlation coefficients of the adsorbent, among the two-parameter models, the Langmuir isotherm model and among the three-parameter isotherms, the Redlich-Peterson model had higher R^2. This indicates that the surface of the adsorbent is more closed with the adsorption process and impact of other side factors reduces on metal ion adsorption.

According to what has been said, the adsorption of nickel, cadmium and lead ions on the studied adsorbent is monolayer type.
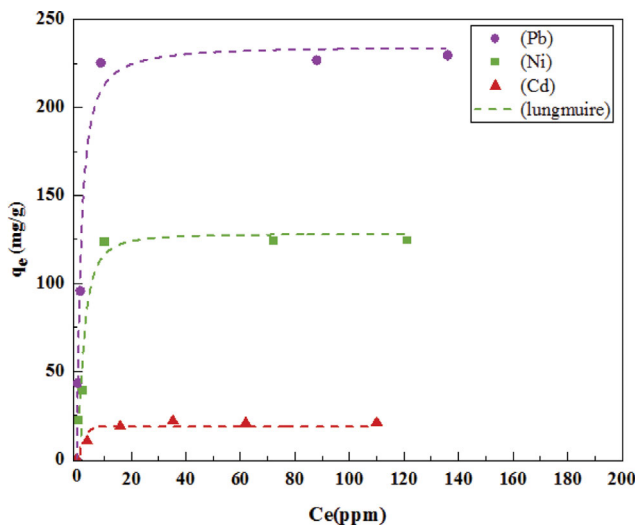
Fig. 12. Langmuir isotherm model for Pb^{+2}, Ni^{+2} and Cd^{+2} adsoption (Initial concentration of ions: 50-200 mg/l, weight of adsorbent: 0.025 g, volume: 35 mL, contact time: 120 min, pH 8, r.t).

Fig. 13. Plot of van't Hoff equation.

The adsorbent structure is homogeneous and has the same adsorption energy. Adsorption has also taken place in both physical and chemical forms. Due to the closeness of the β value in the Redlich-Peterson equation to the number 1, the Langmuir model is more consistent with the experimental equilibrium data. Fig. 12 shows the Langmuir model curve.

1. Adsorption Thermodynamics

Temperature is one of the important parameters affecting the adsorption capacity during the adsorption process. The thermodynamic parameters of the adsorption process such as enthalpy (ΔH^o), entropy (ΔS^o) and Gibbs free energy (ΔG^o) can be defined from the van't Hoff equation [30]. It shows that a plot of lnK vs. 1/T should be a line with slope $-\Delta rH^o/R$ and intercept $\Delta rS^o/R$ (Fig. 13).

The trend in the Gibbs free energy (Table 6) shows negative values for all of the tested metal ions, which indicates that the adsorption process of these metal ions was spontaneous. A positive or a negative change in enthalpy expresses whether a reaction is endothermic or exothermic. Most of the metal ions showed positive ΔH values, indicating that their adsorption was endothermic. The activation energy (E_a) from Dubinin-Radushkevich (D-R) Isotherm values obtained in Table 5 shows that most of the metal ions were adsorbed via physisorption. A reaction is classified as physisorption when the E_a ranges are between 5 and 40 kJ·mol^{-1}, whereas chemisorption has an E_a value between 40 and 800 kJ·

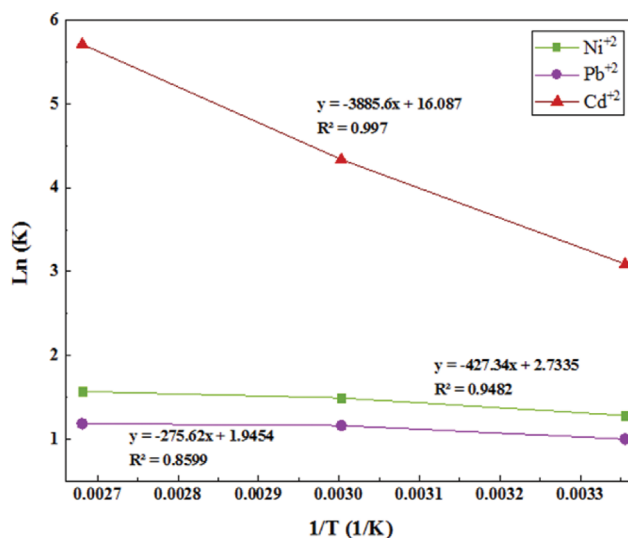**Fig. 14. Proposed mechanism of metal ion adsorption onto Fe$_3$O$_4$@ SiO$_2$@CPTMS@MBOL.**

mol^{-1} [31]. Also, the range of these free energies is larger about -20 kJ/mol and it can be concluded that these adsorptions are physical and there are no strong bonds between the metal ions and the adsorbent.

Table 6. Thermodynamic parameters of the adsorption process

ΔG (KJ/mol)			E_a (KJ/mol)	ΔH (kJ/mol)	ΔS (J/mol/K)	Thermodynamic parameter	
Temperature (^{o}K)							
298	333	273					Pollutants
−3.17	−4.12	−4.86	1.91	3.55	22.72	Ni^{+2}	
−2.47	−3.21	−3.67	2.19	2.29	16.17	Cd^{+2}	
−7.65	−12.0	−17.71	1.52	32.30	133.75	Pb^{+2}	

ADSORPTION MECHANISM

In this study, model of isotherm and kinetic data illustrated that both physical and chemical adsorption would have progressed for the metal ion adsorption onto Fe$_3$O$_4$@SiO$_2$-CPTMS-MBOL. The main steps of adsorption process in the removal of heavy metal ions can be suggested as follows:

• One step is adsorption of ingoing particles onto the external surface of the sorbent via formation of complex or electrostatic attractions.

• Another step can occur through intra-particle penetration due to size of cavities and special surface (BET analysis results and pore size) for a small amount of pollutants on the external surface.

• Ion exchange can be done in the system between hydrogen surface of the hydroxyl groups on the adsorbent and metal ions.

ACTIVITY COMPARISON OF NANO-ADSORBENT

Due to the core-shell structure of the adsorbent, the specific surface area has a small level compared to the other types of adsorbents, but the adsorbent has an acceptable adsorption capacity due to different interactions in comparison with the mentioned references and can be said that the adsorption of pollutants has been done physically, chemically and in a single layer. Table 7 shows the

Table 7. The comparative adsorption capacity of some different adsorbents with proposed for Pb^{+2} ion

Method	Adsorption capacity (mg/g)	Ref.
RB-MMNPs	79.3	32
Nanometer TiO$_2$-DZ	22.5	33
MMWCN	9.3	34
Oiltea shell (OTS)	4.17	35
Modified nanometer SiO$_2$	6	36
Sulfuric acid-treated wheat bran	55.56	37
Amino functionalized mesoporous and nanomesoporous silica	57.74	38
c-MPTMS-SCMNPsb	70.4	39
Fe$_3$O$_4$@SiO$_2$@CPTMS@MBOL	238.4	Present work

comparison of the previous methods used for Pb^{+2} ion removal with our method. In general it can be declared by the present study by reasonable adsorption capacity will be a useful adsorbent.

SELECTIVITY OF NANO ADSORBENT

To evaluate the selectivity of nano adsorbent, a survey was car-

Table 8. Adsorption percentage inorganic ions in two standard solutions by using nano adsorbent

	Entry	Ions	Standard 1: (RTC)	Standard 2: MOO8	Entry	Ions	Standard 1: (RTC)	Standard 2: MOO8
	1	Li	53.5	-	27	Nb	-	-
	2	B	-	-	28	Te	-	-
	3	Be	56.3	-	29	Se	-	-
	4	Na	-	-	30	La	-	-
	5	Mg	98.15	-	31	Ge	-	-
	6	Al	-	34.5	32	Ce	-	-
	7	K	-	-	33	Pr	-	-
	8	Ca	99	97.53	34	Nd	-	-
	9	Ti	93.2	-	35	Sm	-	-
	10	V	66	-	36	Tb	-	-
	11	Cr	71	62	37	Th	-	-
	12	Mn	26.75	24.9	38	U	-	-
Adsorption (%)	13	Co	22.25	34.75	39	Bi	-	-
	14	Ni	71	85	40	Ir	-	-
	15	Cu	-	67.7	41	Os	-	-
	16	Zn	-	39.2	42	Re	-	-
	17	As	10.6	37	43	Hg	-	-
	18	Se	96.7	80	44	Ag	-	-
	19	Sr	97.2	99	45	W	-	-
	20	Mo	95.6	84.7	46	Yb	-	-
	21	Ag	85.81	-	47	pt	-	-
	22	Cd	10.21	-	48	Th	-	-
	23	Sb	76	25.40	49	Hf	-	-
	24	Ba	70.29	-	50	sn	-	-
	25	Pb	93	75	51	s	-	-
	26	Zr	-	-			-	-
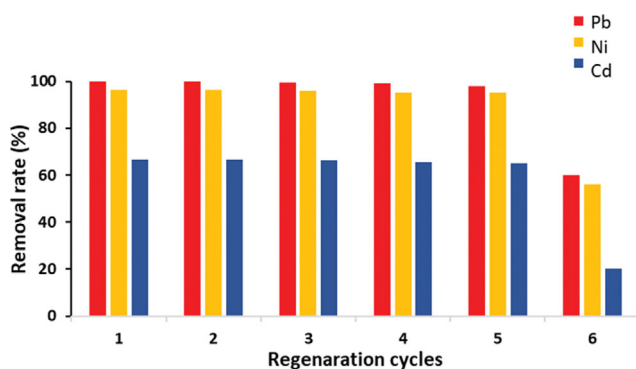
Fig. 15. Reusability of Fe₃O₄@SiO₂@CPTMS@MBOL for the adsorption capacity of for Pb^{2+}, Ni^{2+} and Cd^{2+}.

ried on by Khorasan Razavi Water & Waste Water Company in two types of standard solutions containing fifty inorganic cations and anions in ppb concentration. Due to limitation of detection for some ion concentrations by atomic adsorption instrument, we obtained the results as below (Table 8). The adsorption percentages in presence of different ions illustrate that the designed adsorbent can be used as a cost-effective nontoxic material for industrial issues.

REUSABILITY OF NANO ADSORBENT

To investigate the reuse performance of the nano adsorbents containing Pb^{2+}, it was washed with HNO₃ solution (0.01 M). pH value was adjusted between 2 and 3 until no metal ions were detected in the wash water, as confirmed by the ICP test. Then nano adsorbent was thoroughly washed with deionized water until the pH range of the wash water reached about 5.0-6.5. Afterward, the washed nano adsorbent was dried at 70 °C for 24 h and re-used at least five times for the next removal processes without any significant loss in the adsorption performance (99.9%, 99.9%, 99.5%, 99.1%, 98% respectively). For the Ni^{2+} and Cd^{2+} the process was done the same way as Pb^{2+} and Fe₃O₄@SiO₂@CPTMS@MBOL recovered and reused five times (Fig. 14). In the sixth cycle we observed that the adsorption performance decreased for all metal ions, which may result for the reason of saturation in accordance of irreversible chemical adsorption, the efficiency of adsorbent decreased.

CONCLUSION

This study, by a novel treatment technique, highlights the effectiveness of Fe₃O₄@SiO₂-CPTMS-MBOL adsorbent for the removal of Pb^{2+}, Ni^{2+} and Cd^{2+} ions from water sample in wastewater remedy. To obtain the best results the adsorption process was evaluated in optimized conditions for Pb^{2+}, Ni^{2+} and Cd^{2+} solutions. The Freundlich and Langmuir adsorption isotherms were applied to investigate the adsorption behavior. The high connection items of Langmuir model ($R^{+2}>0.9$) reveal that the Langmuir model offer a reasonable fixation to the experimental data, and so the type of adsorption of Ni^{2+}, Pb^{2+} and Cd^{2+} ions on the Fe₃O₄@SiO₂@CPTMS@MBOL is more agreeable with Langmuir model, where maximum adsorption capacity for Pb^{2+}, Ni^{2+} and Cd^{2+} ions was 238.4, 203.2 and 22.37 mg g⁻¹. Langmuir model is an obvious description for the adsorption procedure.

This proposed inexpensive procedure opens an accessible approach to exploit from different organic ligands for modification of magnetic nanoparticles due to applying as a replacement recyclable adsorbent for the reduction or removal of some cations and anions from water samples.

REFERENCES

1. Y. Sun, K. J. Shah, W. Sun and H. Zheng, *Sep. Purif. Technol.*, **215**, 208 (2019).
2. S. Muthusaravanan, N. Sivarajasekar, J. S. Vivek, T. Paramasivan, M. Naushad, J. Prakashmaran, V. Gayathri and O. K. Al-Duaij, *Environ. Chem. Lett.*, **16**, 1339 (2018).
3. K. Rambabu, A. Thanigaivelan, G. Bharath, N. Sivarajasekar, F. Banat and P. L. Show, *Chemosphere*, **268**, 128809 (2021).
4. K. Janani, N. Sivarajasekar, S. Muthusaravanan, K. Ram, J. Prakashmaran, S. Sivamani, N. Dhakal, T. Shahnaz and N. Selvaraju, *Bioresour. Technol.*, **7**, 100265 (2019).
5. V. J. Sharavanan, M. Sivaramakrishnan, N. Sivarajasekar, N. Senthilrani, R. Kothandan, N. Dhakal, S. Sivamani, P. L. Show, M. R. Awual and M. Naushad. *Environ. Chem. Lett.*, **18**, 325 (2020).
6. S. Muthusaravanan, N. Sivarajasekar, J. S. Vivek, S. V. Priyadharshini, T. Paramasivan, N. Dhakal and M. Naushad, *Green Materials for Wastewater Treatment*, **38**, 191 (2020).
7. B. M. Jun, N. Her, C. M. Park and Y. Yoon, *Environ. Sci. Water Res. Technol.*, **6**, 173 (2020).
8. M. Corral Bobadilla, R. Lostado Lorza, F. Somovilla Gómez and R. Escribano García, *Water*, **12**, 1320 (2020).
9. C. P. Devatha and S. Shivani, *J. Environ. Manage.*, **258**, 110038 (2020).
10. A. Azimi, A. Azari, M. Rezakazemi and M. Ansarpour, *ChemBioEng Rev.*, **4**, 37 (2017).
11. M. M Rahman, M. Asaduzzaman and R. Naidu, *J. Hazard. Mater.*, **262**, 1056 (2013).
12. M. Anjum, R. Miandad, M. Waqa, F. Gehany and M. A. Barakat, *Arab. J. Chem.*, **12**, 4897 (2019).
13. L. C. Lin, J. K. Li and R. S. Juang, *Desalination*, **225**, 249 (2008).
14. H. L. Fan, S. F. Zhou, W. Z. Jiao, G. S. Qi and Y. Z. Liu, *Carbohydr. Polym.*, **174**, 1192 (2017).
15. H. Bessbousse, T. Rhlalou, J. F. Verchère and L. Lebrun, *J. Member. Sci.*, **307**, 249 (2008).
16. Y. Benito and M. L. Ruiz, *Desalination*, **142**, 229 (2002).
17. F. Zhao, W. Z. Tang, D. Zhao, Y. Meng, D. Yin and M. Sillanpää, *J. Water Process Eng.*, **4**, 47 (2014).
18. M. Kobya, E. Demirbas, E. Senturk and M. Ince, *Bioresour. Technol.*, **96**, 1518 (2005).
19. P. Panneerselvam, V. Bala, N. Thinakaran, P. Baskaralingam, M. Palanichamy and S. Sivanesan, *E- J. Chem.*, **6**, 729 (2009).

20. M. Q. Jiang, X. Y. Jin, X. Q. Lu and Z. L. Chen, *Desalination*, **252**, 33 (2010).
21. R. D. Ambashta and M. Sillanpää, *J. Hazard. Mater.*, **180**, 38 (2010).
22. Y. C. Sharma, V. Srivastava, V. K. Singh, S. N. Kaul and C. H. Weng, *Environ. Technol.*, **30**, 583 (2009).
23. B. R. White, B. T. Stackhouse and J. A. Holcombe, *J. Hazard. Mater.*, **161**, 848 (2009).
24. Y. C. Sharma and V. Srivastava, *J. Chem. Eng. Data*, **55**, 1441 (2010).
25. H. Karami, *Chem. Eng. J.*, **219**, 209 (2013).
26. A. Z. M. Badruddoza, Z. B. Z. Shawon, W. J. D. Tay, K. Hidajat and M. S. Uddin, *Carbohydr. Polym.*, **91**, 322 (2013).
27. M. Ariannezhad, D. Habibi and S. Heydari, *Russ. J. Org. Chem.*, **55**, 1591 (2019).
28. S. J. Hawkes, *J. Chem. Educ.*, **73**, 516 (1996).
29. H. Watanabe and J. E. Seto, *Bull. Chem. Soc. Jpn.*, **59**, 2683 (1986).
30. R. Pirarath, P. Shivashanmugam, A. Syed, A. M. Elgorban, S. Anan-dan and M. Ashokkumar, *Front Environ. Sci. Eng.*, **15**, 1 (2021).
31. H. K. Boparai, M. Joseph and D. M. O'Carroll, *J. Hazard. Mater.*, **186**, 458 (2011).
32. T. Madrakian, A. Afkhami and M. Ahmadi, *Chemosphere*, **90**, 542 (2013).
33. N. Lian, X. Chang, H. Zheng, S. Wang, Y. Cui and Y. Zhai, *Microchim. Acta*, **151**, 81 (2005).
34. S. Mohammadi, D. Afzali and D. Pourtalebi, *Open Chem.*, **8**, 662 (2010).
35. J. Liu, C. Hu and Q. Huang, *Bioresour. Technol.*, **271**, 487 (2019).
36. Y. Cui, X. Chang, Y. Zhai, Z. H. Zhu and N. Lian, *Microchem. J.*, **83**, 35 (2006).
37. A. Ozer, *J. Hazard. Mater.*, **141**, 753 (2007).
38. A. Heidari, H. Younesi and Z. Mehraban, *Chem. Eng. J.*, **153**, 70 (2009).
39. C. Huang and B. Hu, *Spectrochim. Acta Part B.*, **63**, 437 (2008).